King Saud University

Arabian Journal of Chemistry

www.ksu.edu.sa
www.sciencedirect.com

ORIGINAL ARTICLE

Robust interface on ENR-50/TiO₂ nanohybrid material based sol-gel technique: Insights into synthesis, characterization and applications in optical

Omar S. Dahham *, Nik Noriman Zulkepli

Center of Excellence Geopolymer and Green Technology, Faculty of Engineering Technology, Universiti Malaysia Perlis, 02100 Padang Besar, Perlis, Malaysia

Abstract   In this work, the sol–gel technique was used to prepare a new organic–inorganic hybrid from Epoxidized Natural Rubber (ENR-50) and Titanium dioxide (TiO₂) by blending different content of titania precursors (10, 30, and 50 wt%) with an ENR-50 matrix. A wide range of analyses was conducted to understand the nature of this hybrid and also to evaluate its potential uses in applications required high refractive index such as micro optical and optoelectronic devices. Results indicated that the ring-opening reaction of epoxide groups in ENR-50 increased with the increase of titania content in the hybrid resulting a strong bonding between titania and ENR-50 through Ti—O—C bond, which was observed in FTIR spectrum at 1027–1028 cm^{-1}. It is also observed a slight decrease in the intensity of the amorphous peak along with a new crystalline peak appeared at $2\theta = 23$ and 27° due to the crystalline nature of titania. The hybrids showed three thermal degradation steps in the range of temperature 76 to 769 °C due to the existence of the Ti moieties with the mixture of polymer chains, which in turn shifted the T_g at 24.3, 26.9 and 28.1 °C for the hybrid at 10, 30, and 50 wt% TiO₂ compared to the T_g of ENR-50 at −18.4 °C respectively. The morphology of the ENR-50 showed clear changes during of the synthesis of ENR-50/TiO₂ hybrids, these changes were proven by SEM, TEM, and AFM analyses. Uv–Vis results showed that the higher

* Corresponding author.
  E-mail addresses: eng.omar@mail.com (O.S. Dahham), niknoriman
@unimap.edu.my (N.N. Zulkepli).
Peer review under responsibility of King Saud University.

ELSEVIER | **Production and hosting by Elsevier**

wavelength peak at 293 nm has shifted to 296, 298 and 300 nm for the hybrid at 10, 30, and 50 wt% TiO$_2$ respectively due to the strong interaction between titania precursors and ENR-50 matrix. Furthermore, the hybrids showed good optical transparency in the visible light range.

1. Introduction

The improvements on the materials used in optical applications have become necessary due to the rapid development in the advanced optical devices (Higashihara and Ueda, 2015). In the last few years, the polymeric materials were extensively developed and utilized in microoptic and optoelectronic applications, such as encapsulants for light-emitting diode devices, advanced display devices, plastic lenses for projector, camera and eyeglasses, and microlens components for complementary metal oxide semiconductor image sensors as alternatives for inorganic optical materials (Cui et al., 2001; Olshavsky and Allcock, 1995; Ma et al., 2002; Burroughes et al., 1990). However, polymeric materials possess some limitations in optical properties due to their intrinsic organic nature, which cause a relatively low refractive index (in the range of 1.3–1.7) (Olshavsky and Allcock, 1995; Zimmennann et al., 1993). Therefore, adding second material is essential for improving their properties and applications. In the last few decades, the preparation of organic/inorganic hybrids has attracted much attention due to their combined properties of organic polymers and inorganic materials. These hybrids combine the advantages of organic polymers (flexibility, lightweight, good processability, and good impact resistance) and inorganic materials (high brittleness, high thermal stability, and good chemical resistance) (Moore et al., 2012; Tanaka and Kozuka, 2004), which in turn allow these materials to use in numerous applications such as optical coatings, nonlinear optical devices (Wang et al., 1991), light emitting diodes (Ju et al., 2006); photoresponsive devices (Wang et al., 2010), and also in medical applications (Drisko and Sanchez, 2012).

One of the most considerable metal oxides used as inorganic material in organic/inorganic hybrids is the Titanium dioxide (TiO$_2$), which shows a high refractive index (RI) and offers a promising platform for optical applications (Macwan et al., 2011). Unfortunately, the high density along with the low flexibility of TiO$_2$ may limit its uses in optical and other applications. However, in presence of polymers, high refractive index hybrids were successfully and used in optical applications (Macwan et al., 2011) In particular, Titanium dioxide (TiO$_2$), as inorganic material, was added into a polymer matrix to synthesize high refractive index hybrids using sol–gel technique (Liu and Ueda, 2009). Different types of polymer/TiO$_2$ hybrids, such as poly(arylene-ether-sulfone)/TiO$_2$ (Wang et al., 1991), poly(arylene-ether-ketone)/TiO$_2$ (Wang et al., 1991); aminoalkoxysilane capped-pyromellitic dianhydride/TiO$_2$ (Chang and Chen, 2001) and poly(methylmethacrylate)/TiO$_2$ (Lee and Chen, 2001), Polyimide/TiO$_2$ (Su and Chen, 2008); polysilsesquioxanes/TiO$_2$ (Chen et al., 2004), Epoxy/TiO$_2$ (Guan et al., 2006) and others (Di Gianni et al., 2007) have been studied using this technique. Furthermore, the optical, thermal and mechanical properties of the hybrids can be easily adjusted via manipulating the ratio of inorganic phase to organic phase. The properties of the hybrids are not only relative to the properties of each phase, but also to the interfacial properties and phase morphology of the hybrid. Thus, the control of phase separation and morphology are essential in the research for inorganic/organic hybrids (Dou et al., 2015). The interfacial force between inorganic and organic phases plays an important role in controlling microstructure and properties of hybrids. The formation of covalent bonds (Peng, 2004) and/or hydrogen bonds (Aakeröy et al., 1999) between inorganic and organic materials can prevent or significantly reduce the phase separation.

Epoxidized natural rubber (ENR) is a modified natural rubber (NR) produced by epoxidation process of NR with acetic peroxide or formic peroxide in a reactor (Gelling et al., 1991; Hamzah et al., 2012). ENR contains two different functional groups, epoxides (E) and alkenes (C) that randomly distributed in its backbone (Hamzah et al., 2012; Gan and Hamid, 1997). 3;4 Epoxide rings are the reactive sites of the E groups, which involved with the ring opening reaction whereas the double bonds are the reactive sites for C groups, which are involved with crosslinking reaction (Ratnam et al., 2000a, 2000b, 2001c; Akiba and Hashim, 1997). The type of polymer contains two different reactive sites incorporating with nanoscale inorganic moieties can offer a high possibility of producing transparent hybrids with improved thermal and other properties. (Hamzah et al., 2012; Salaeh and Nakason, 2012). There are only very few studies can be found on the synthesis of hybrids from ENR as a host organic polymer. For instance, Mahmood et al., have successfully synthesized hybrid films from ENR-50 and zirconia precursors by using sol–gel processing (Mahmood et al., 2013). It is found that the possible interaction between ENR-50 and zirconia precursors increased as precursors increase. Furthermore, the hybrids showed improvements in the thermal stability and optical transparency as compared to pure ENR-50. Another research done by Tan and Bakar, reported a simple in situ synthesis of ENR/iron oxide (magnetite) nanocomposites (Tan and Bakar, 2013). Results suggested that no chemical interactions between ENR and magnetite. However, the electrical conductivity of the nanocomposites improved as magnetite content increase.

Our previous reports investigated the influences of different mediums on the structural properties of ENR-50/TiO$_2$ hybrid using 1D/2D NMR technique (Dahham et al., 2018). We found that the presence of these mediums; particularly acetic acid (Dahham et al., 2018) has significantly increased the ring-opening reaction of epoxide groups in ENR-50 and covalently bonded with Ti precursors forming Ti─O─C. However, these reports were limited to the study of ENR-50/TiO$_2$ hybrid structure. To the best of our knowledge, there is no report gave a complete assignment on the properties of ENR-50/TiO$_2$ nanohybrid. Therefore, it is important to extent the investigation on this hybrid as this understanding is essential for theoretical and application point of view.

In this work, we have successfully synthesized a new hybrid from ENR-50 and titania precursors using sol–gel technique. This hybrid was characterized via a wide range of analysis such as fourier transform infrared spectroscopy (FTIR), x-ray diffraction (X-RD), thermal gravimetric analysis (TGA), differential scanning calorimetry (DSC), scanning electron microscopy (SEM), energy-dispersive x-ray (EDX), transmission electron microscopy (TEM), atomic force microscopy (AFM), ultraviolet–visible (UV–vis) microscopy, and refractive index (RI) measurement.

2. Experimental

2.1. Materials

The epoxidized natural rubber (ENR-50) was obtained from the Rubber Research Institute, Kuala Lumpur, Malaysia. Titania precursors (Titanium (IV)-isoproproxide 98%) were purchased from Merck, Germany. Other chemicals (toluene, chloroform, tetrahydrofuran, n-hexane, and 2-propanol, were purchased from Systerm, Malaysia, and used as they are without any further purification.

2.2. Hybrid preparation method

All experiments were carried out at atmospheric pressure. The synthesis process of the ENR-50/TiO$_2$ hybrid included two main stages:

2.2.1. ENR-50 purification

Purification process of ENR-50 was conducted by dissolving 20 g of ENR-50 in 400 mL chloroform and then stirring for 24 h at 25 °C (Dahham et al., 2018). After that, the mixture was filtered through a pack of cotton gauze to separate the high molecular weight from the low molecular weight ENR-50. The last was precipitated after the addition of n-hexane. The precipitate was moved into a Teflon petri dish and kept at room temperature for 48 h. Further drying on the sample was conducted using vacuum oven at 50 °C for 24 h. Once dry, the sample represented the purified ENR-50 (Dahham et al., 2018).

2.2.2. ENR-50/Titania hybrids synthesis

The organic/inorganic hybrids can be synthesized using different sol–gel routs (Rawolle et al., 2012). In this work, ENR-50/TiO$_2$ at 10 wt% of titani, Ti(OCH$_2$CH$_2$CH$_3$)$_4$ solution was prepared by adding a 38.18 mg (1.32×10^{-4} mol) of Ti(OCH$_2$CH$_2$CH$_3$)$_4$ precursors in 10 mL Isopropanol. Then, about 10 mL of Ti(OCH$_2$CH$_2$CH$_3$)$_4$ solution was gradually added drop wise to the 44 mL of the purified ENR-50 at 60 °C. The mixture was reserved at 60 °C for 24 h. The rfinal mixture was cast onto petri dish and reserved for normal drying about 48 h. After normal drying, the sample was vacuum at 50 °C for 24 h. The process was repeated with different content of precursors to prepare ENR-50/TiO$_2$ at 30, and 50 wt% of titania.
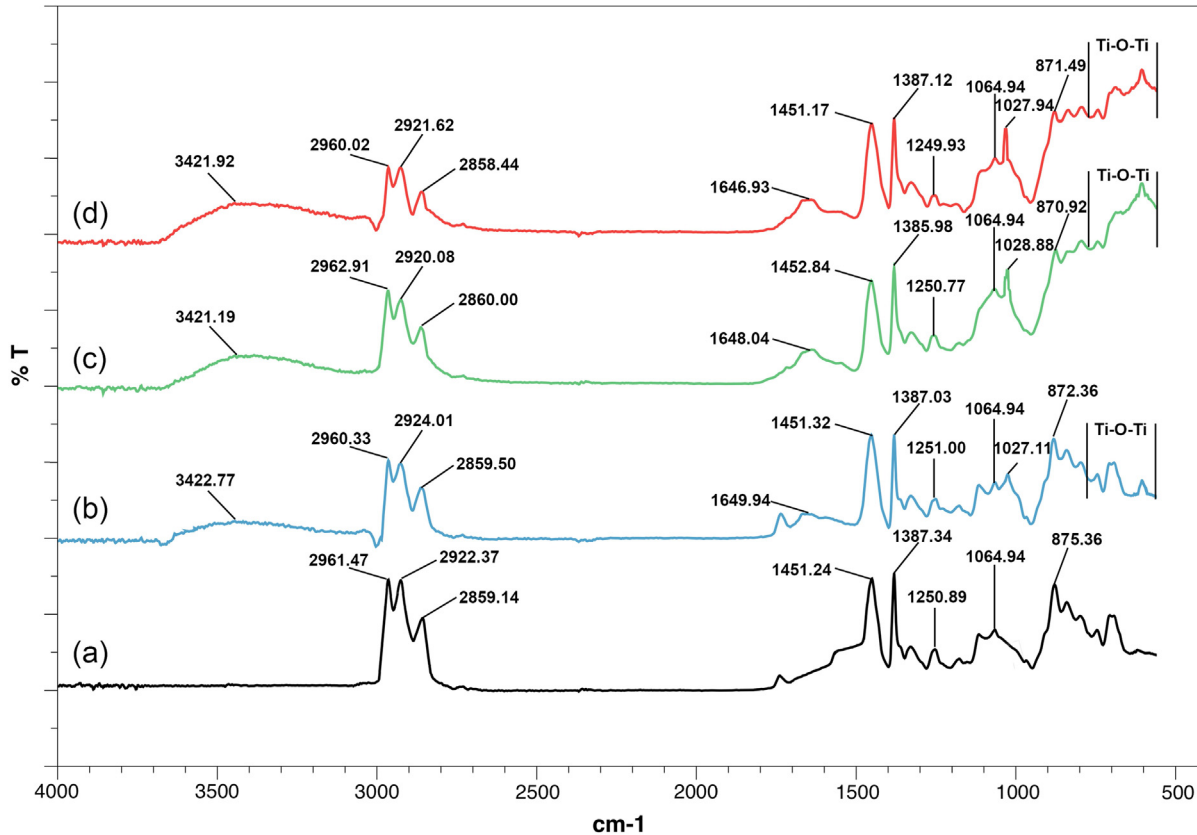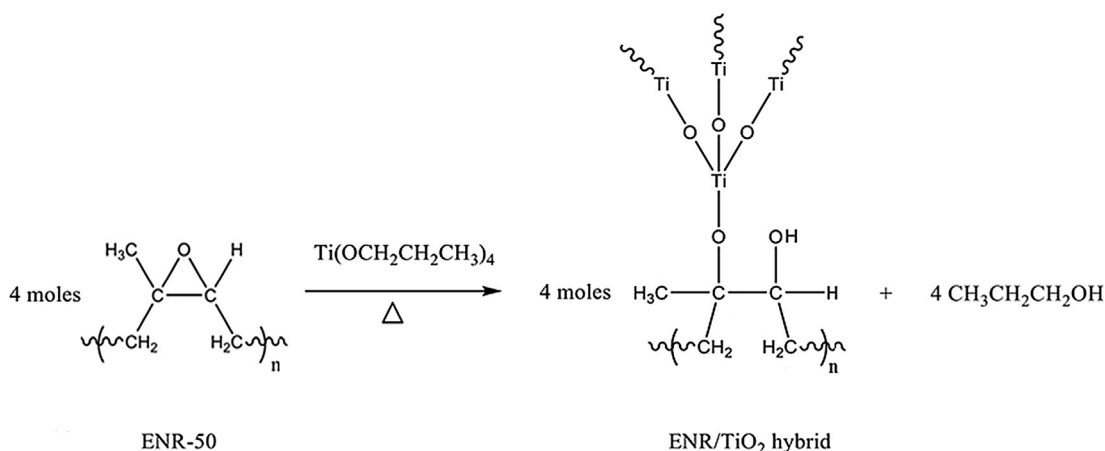

Fig. 1 FTIR spectra of (a) ENR-50, (b) ENR-50/TiO$_2$ 10 wt%, (c) ENR-50/TiO$_2$ 30 wt%, and (d) ENR-50/TiO$_2$ 50 wt%.
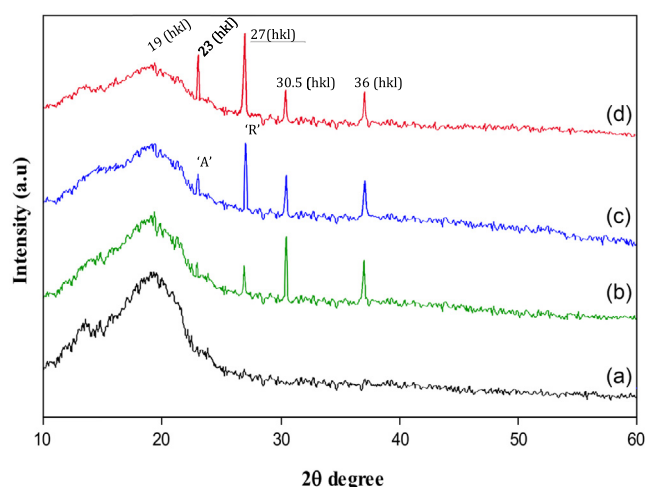
Scheme 1 Proposed possible reaction of ENR-50/TiO$_2$ hybrid.

Fig. 2 XRD pattern of (a) ENR-50, (b) ENR-50/TiO$_2$ 10 wt%, (c) ENR-50/TiO$_2$ 30 wt%, and (d) ENR-50/TiO$_2$ 50 wt%.

2.3. Hybrids characterization

2.3.1. Fourier transform infrared spectroscopy (FTIR)

Transmission FTIR spectra of the hybrids were recorded by Perkin-Elmer 2000-FTIR from single beam transmittance onto a film of the sample on a ZnSe window at room temperature. The samples were scanned from 4000 to 600 cm^{-1} with resolution of 0.4 cm^{-1}. All spectra were subjected into an average of 16 scans for each sample.

2.3.2. X-Ray diffraction (X-RD)

The crystallinity and purity of specimens were evaluated using PANalytical (X'pert PRO) PN 3040/60 XRD, equipped with a monochromatic Cu-Ka radiation filter with wavelength = 0.154 nm. The specimens were scanned in the 2θ range of 5–40° at a scan rate of 4°/min

2.3.3. Thermal gravimetric analysis (TGA)

TGA analysis was performed using a Perkin Elmer TGA-7 1991 analyzer. The specimens were heated from room temperature (about 30 °C) to 900 °C at 20 °C/min a heat rate under a nitrogen flow. The results of TGA and DTG were recorded and analyzed.

2.3.4. Differential scanning calorimetry (DSC)

DSC analysis was conducted using a Perkin Elmer Pyris-6 (Shelton CT). The specimens were sealed in an aluminium pan, and heated from −50 to140 °C at 20 °C/min a heat rate under a nitrogen flow. After that, the temperature was quenched from 140 °C to −50 °C and heated again from −50 to 140 °C at same heat rate. The results of DSC was recorded from the second heating and analyzed.

2.3.5. Scanning electron microscopy/energy-dispersive X-ray (SEM/EDX)

SEM-EDX test was performed using *JEOL JFC6460LA,* operated at 10 kV. Specimens were coated with an extremely thin layer of gold (1.5–3 nm) to prevent the electrostatic charging and also to avoid the poor resolution of the micrographs during test.

2.3.6. Transmission electron microscopy (TEM)

To clarify the nanoscale structure of the hybrids, TEM micrographs were recorded on *Jeol Instrument (JEM-1230)* operated at 20 kV. Specimens were dissolved in analytical grade of tetrahydrofuran (THF). About 2–3 drops of prepared solution was dropped onto a carbon-coated copper grid (200 mesh). The specimens were air dried prior to analysis.

2.3.7. Atomic force microscopy (AFM)

AFM (Veeco di CP-II) was utilized to examine surface topography of the hybrids. The surface of each specimen was scanned at 6 points (2 points at center, 2 points at perimeter and 2 points at half distance between center and perimeter) in contact mode with CONT20A-CP tips. The resolution at 256 × 256 and scan rate at 1 Hz were used to obtain topography on a 3 μm × 3 μm scanning area.

2.3.8. Ultraviolet–visible (UV–vis) microscopy

UV–vis spectrophotometer (Perkin Elmer Lambda 35) was used to evaluate the optical property of the prepared hybrids
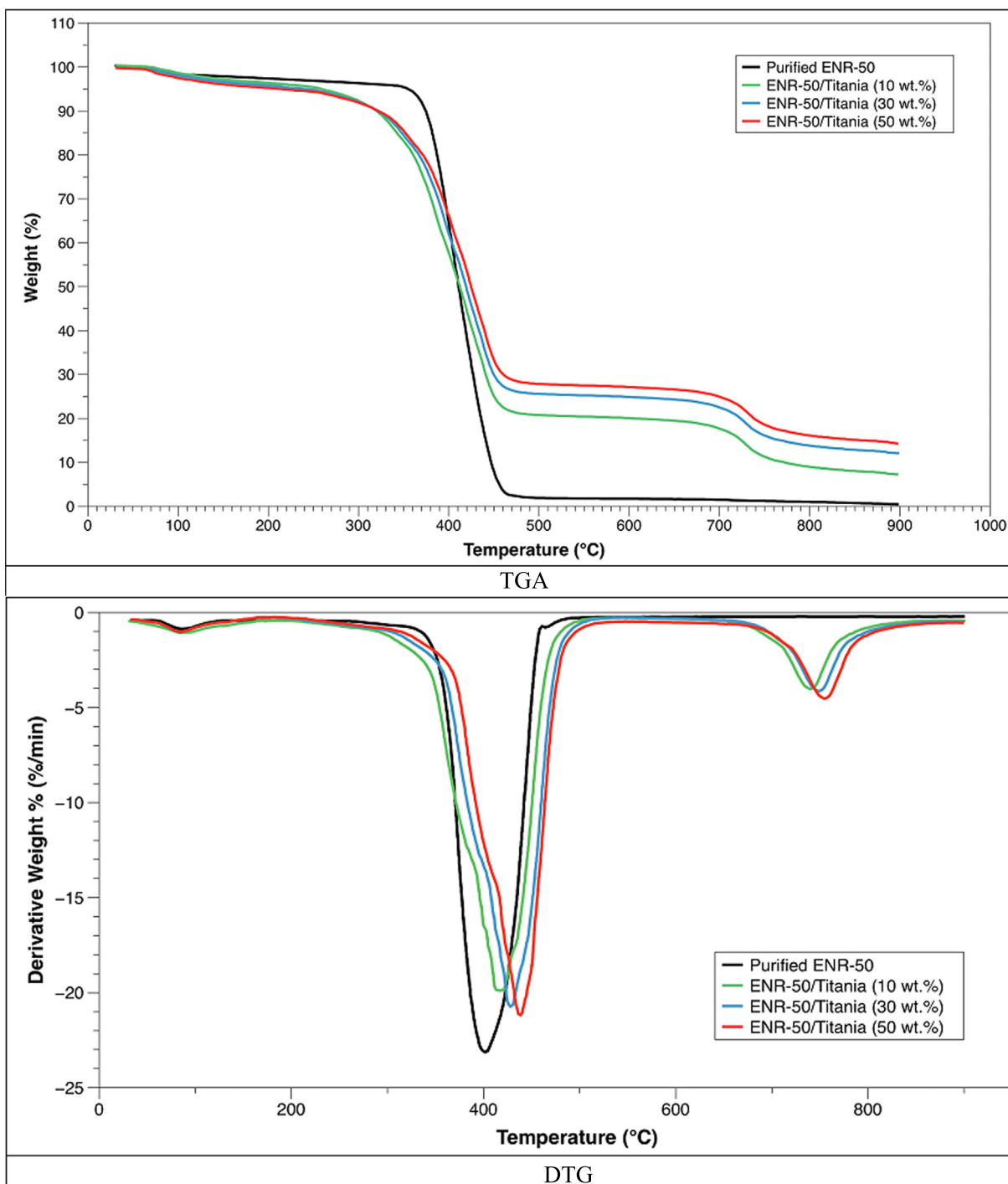
Fig. 3   TGA-DTG thermograms of ENR 50 and ENR-50/TiO$_2$ at difference Ti Content.

in the wavelength range of 200–550 nm and at resolution of 1 nm. The specimens were prepared for the measurements by dissolving them in tetrahydrofuran (THF).

2.3.9. Refractive index (RI) measurement

The RI of the hybrids was measured on an Atago 3261 Automatic Digital RX-5000α Microphotonics Ellipsometer with light source of LED and wavelength of 589 nm. Each specimen was measured five times at the same experimental condition in order to determine the errors of the data.

3. Results and discussion

3.1. Interaction of ENR-50 and titania (FTIR)

Fig. 1 shows the FTIR spectra of purified ENR-50 and the ENR-50/TiO$_2$ hybrids with different titania content at 10, 30 and 50 wt% respectively. The FTIR spectrum of the ENR-50 (Fig. 1a) shows the characteristic band at 870–875 cm^{-1} corresponding to the stretching vibration of epoxy groups (Dahham et al., 2020; Salehabadi et al., 2014). Other charac-

teristic band found at 1064 cm^{-1}, which is belong to the symmetric and asymmetric stretching of C—O groups, and those at 1249–1251 cm^{-1} are belong to epoxy whole ring. The bands identified at 1385–1387 cm^{-1} and 1451–1452 cm^{-1} probably correspond to the deformations of hydrocarbon backbone for CH and CH$_2$ groups, 2858–2860 cm^{-1}, 2920–2924 cm^{-1} and 2960–2962 cm^{-1} due to the CH$_2$ symmetry stretching, CH$_2$ asymmetry stretching, and CH$_3$ stretching respectively (Salehabadi et al., 2014; Hamzah et al., 2016). The spectra of the ENR-50/TiO$_2$ hybrids are shown in Fig. 1b, c, and d respectively. It is observed that the increasing of titania content increased the intensity of broad OH group at 3421–3422 cm^{-1} which is also accompanied by decreasing the intensity of epoxide peak at 870–875 cm^{-1}. This was due to the ring opening reactions (ROR) of epoxide groups in ENR-50. Furthermore, the band at 1646–1649 cm^{-1} is probably belong to the C=O or C—O—C groups, resulting from the ROR of epoxide groups. Another peak was observed at 1027–1028 cm^{-1} due to the Ti—O—C bond in the hybrid (Chen et al., 2007). The broad band at the region of 500–800 cm^{-1} is attributed to Ti—O—Ti and indicates the presence of Ti moieties in the formed hybrid (Yu et al., 2013; Zhang et al., 2012). It is also found that the intensity of these peaks of groups of C=O, C—O—C, Ti—O—C and Ti—O—Ti increased with the increasing of titania content in the hybrids. Therefore, these results indicate that there are interactions between ENR-50 and titania and the maximum interaction occurs with high content of titania (50 wt%).

Scheme 1 showed the proposed possible reaction of ENR-50/TiO$_2$ hybrid. Based on the characteristic bands uncover in the FTIR spectra (Fig. 1), the peak observed at 1027–1028 cm^{-1} is related to the Ti—O—C in the hybrid, resulting

a covalent bond between titanuim and opened epoxy ring. The other peak observed at 3421–3422 cm^{-1}, which is for the hydroxyl group (OH) found in the formed propanol as a side product in the proposed reaction.

3.2. (X-RD) crystallinity of the hybrid

The X-ray diffractograms of purified ENR-50 and the hybrids are sown in Fig. 2. The hybrids showed a new diffraction peak at 2θ = 23 (1 0 1) and 27° (1 1 0) respectively, which represent the anatase 'A' and rutile 'R' phases as marked at the figure. The well-crystallized anatase and rutile forms were observed in the hybrid samples (b, c, and d) indicating successful addition of titani into ENR-50. The intensity of the anatase 'A' and rutile 'R' peaks changed as the titania content change in the hybrids. This is consistent with the study done by Motaung et al. (Motaung et al., 2011), the amorphous peak for the ENR-50 is present in all four the diffractograms at 2θ = 19°. However, a slight decrease in the intensity of the amorphous peak concurrently with a new crystalline peak have developed at 2θ = 23 (1 0 1) and 27° (1 1 0). These observations point to the new diffraction peak development in the ENR-50 matrix that is probably the result of the nanoparticles acting as nucleation centers in the rubber (Motaung et al., 2011).

3.3. Thermal stability (TGA)

TGA DTG thermograms of purified ENR-50 and ENR-50/TiO$_2$ hybrid samples are presented in Fig. 3a and b respectively. It is observed that the purified ENR-50 shows two
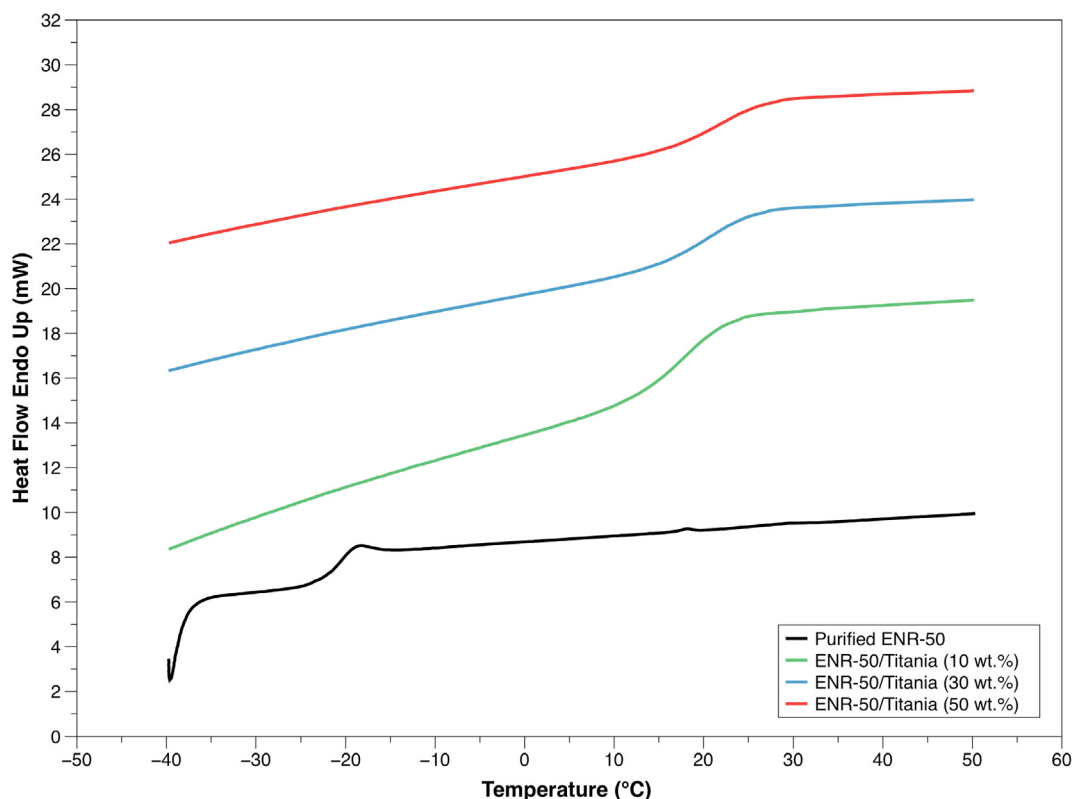

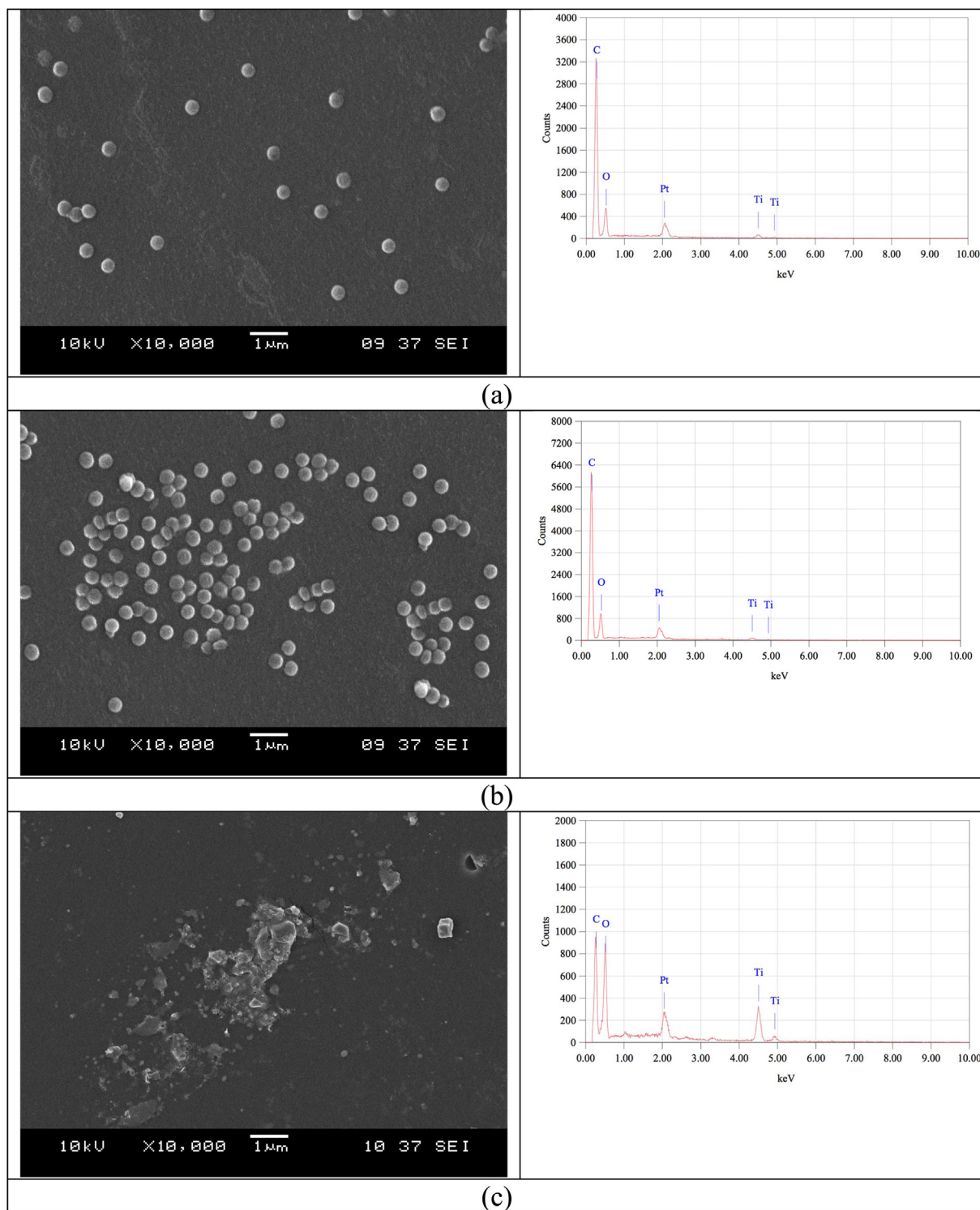**Fig. 4** DSC thermograms of ENR 50 and ENR-50/TiO$_2$ at difference Ti Content.

Fig. 5   SEM- EDX of (a) ENR-50/TiO$_2$ 10 wt%, (b) ENR-50/TiO$_2$ 30 wt%, and (c) ENR-50/TiO$_2$ 50 wt%.

degradation steps at 78–111 °C and 364–474 °C respectively. The first step is attributed to the loss of moisture and also the solvent that may be stuck in the polymer matrix during the purification process. The second step is the maximum degradation peak which is due to the thermal degradation of ENR-50 (Bijarimi et al., 2014).

For all ENR-50/TiO$_2$ hybrids, (10, 30 and 50 wt% Titania addition), three thermal degradation steps were observed in the range of temperature 76 to 769 °C respectively. The first degradation step at 76–134 °C represents the loss of moisture and trapped organic residues from the porous gel network of the formed hybrids (Caldeira et al., 2012). The second degradation
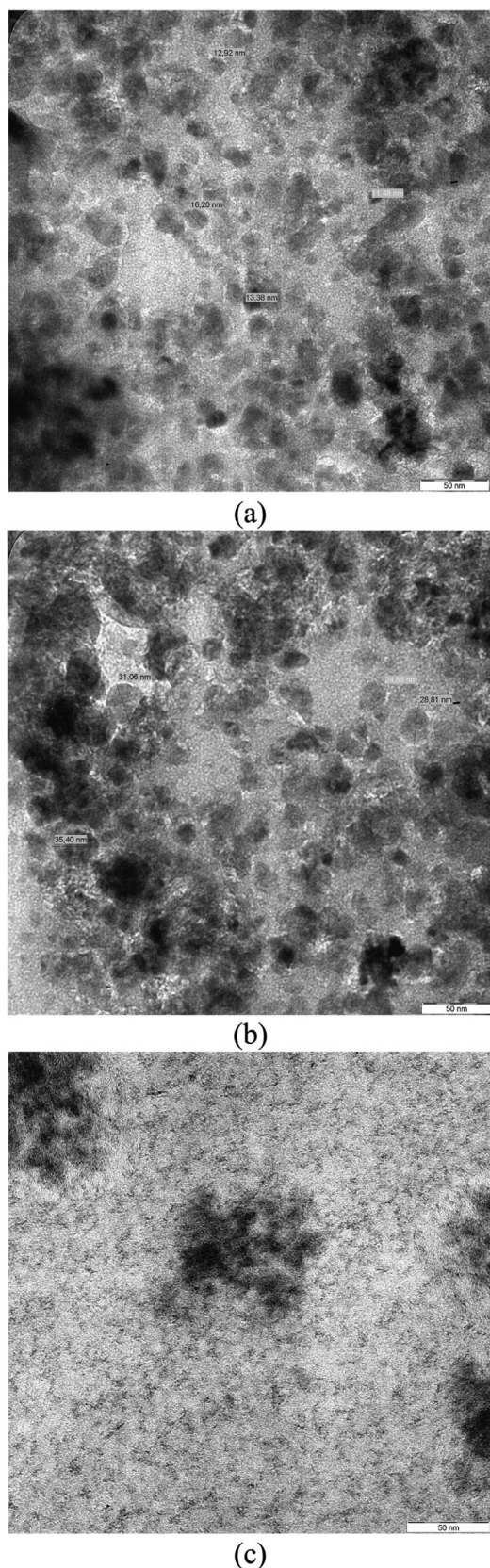
Fig. 6 TEM micrographs of (a) ENR-50/TiO₂ 10 wt%, (b) ENR-50/TiO₂ 30 wt%, and (c) ENR-50/TiO₂ 50 wt%.

step at 254–482 °C represents the degradation of the majority of the ENR-50 matrix. This degradation is shifted to a higher temperature compared to the purified ENR-50. During the pyrolysis process of ENR-50, there are few possibilities of degradation may occur such as an elimination reaction of certain organic groups, breakdown of the main chains of polymer, and de-polymerization (Schnabel, 1981). Typically, low molecular weight organic molecules are stable at temperature range of 100–200 °C (Schnabel, 1981; Brown, 2001), and requires low heat energy to break up its bond (Li et al., 1998). However ENR chain distributes its energy along the polymer chains, thus it is able to stabilize its chains up to higher temperature as compared with the simple organic molecules (Schnabel, 1981). The third degradation step at 691–769 °C represents the re-arrangement of Ti—O—Ti skeleton to a discrete TiO₂ peroskite structure. On the other hand, it can be observed that there was an improvement on the degradation temperature of ENR-50/TiO₂ hybrids compared to the purified ENR-50. Furthermore, the degradation temperature of the hybrids increased with the increase of titania addition to the ENR-50. The reason behind these results is attributed to the protective effect of titania network against organic ENR-50 matrix.

3.4. DSC study

DSC thermograms of purified ENR-50 and the ENR/TiO₂ hybrids at 10, 30 and 50 wt% of titania are shown in Fig. 4. It is observed that the hybrids at 10, 30, and 50 wt% of titania show a single glass transition (Tg) at 24.3, 26.9 and 28.1 °C respectively, which are higher than the T_g of purified ENR-50 at −18.4 °C (Çopuroğlu et al., 2006; Morselli et al., 2012). The single T_g indicates the robust interface between the ENR-50 matrix and the titania moieties (Morselli et al., 2012). Furthermore, the single T_g value indicates the hybrids acts as a new polymer (Mas Haris and Raju, 2014). Our earlier studies found that the percentage of ring opening reaction (ROR) of epoxide units in the ENR-50 hybrid has a direct influence on the T_g value of the ENR-50/TiO₂ hybrid (Dahham et al., 2018). The Ti moieties are able to restrict the movement of polymer chains via crosslinking in the hybrid. Therefore, the hybrids remain rigid at higher temperatures as compared with the purified ENR-50. However, the hybrids remain in a glassy phase below the T_g and a rubbery phase above the T_g.

The content of Ti contributes to the free volume of the polymers. Free volume is the space existing between the chains of the polymer, this space can be measured by positron annihilation method. Free volume varies as the molecules oscillate. Also, the free volume decreases as the intermolecular cohesion increases. Thus, the high Ti content in the ENR-50/TiO₂ hybrid reduce the free volume and restrict the movement of the polymer chains, whereas the polymer chains have high free volumes at low Ti content and they can move easily.

3.5. Morphology and dispersibility of ENR-50/TiO₂ hybrid

SEM and TEM analyses were conducted in order to examine the microstructures and the distribution of TiO₂ nanoparticles
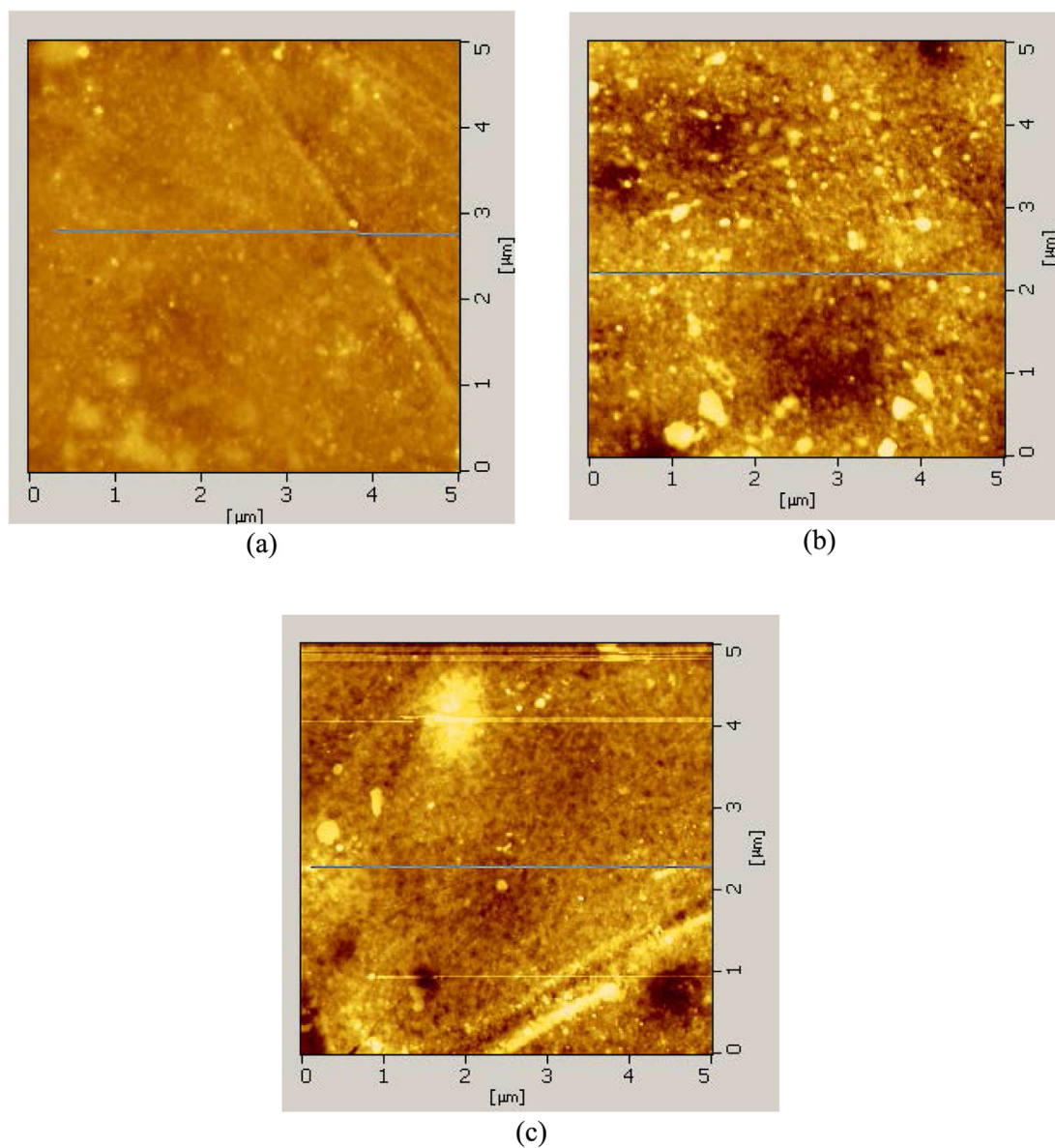
Fig. 7   AFM images of (a) ENR-50/TiO$_2$ 10 wt%, (b) ENR-50/TiO$_2$ 30 wt%, and (c) ENR-50/TiO$_2$ 50 wt%.

within the hybrid, while EDX analysis was conducted to identify the TiO$_2$ nanoparticles in the hybrids. Typical SEM-EDX micrographs of the ENR-50/TiO$_2$ hybrids at 10, 30, and 50 wt % titania are illustrated in Fig. 5a, b, and c respectively. It can be observed that the lower content of TiO$_2$ nanoparticles, particularly 10 wt% TiO$_2$ was evenly distributed in the ENR-50 matrix (Fig. 5a) indicating that the TiO$_2$ nanoparticles had a strong interfacial bonding and excellent adhesion to the ENR-50 matrix. It is also worthily to mention that the morphology of the ENR-50 was changed during of the synthesis of ENR-50/TiO$_2$ hybrids. By increasing the titania content up to 30 wt% (Fig. 5b), the distribution of nanoparticles remained good enough. However, the higher content of titania (50 wt% TiO$_2$) showed severe agglomerations of the nanoparticles (Fig. 5c) and it became difficult to distinguish the spherical shape structures of the TiO$_2$ nanoparticles. Mahmood et al., (Mahmood et al., 2013) found the same behavior of the zirconia nanoparticles within the ENR-50 matrix, which are homogeneously and uniformly distributed throughout the

ENR-50 matrix as low content of zirconia used while they are being severely agglomerated in the ENR-50 matrix as high content of zirconia used. EDX analyses of the ENR-50/TiO$_2$ hybrids confirm the presence of TiO$_2$ nanoparticles their hybrids, the hybrid at higher titania content showed higher intensity peak in EDX figures.

TEM analysis has proven to be a powerful tool to evaluate the size of the TiO$_2$ nanoparticles as well as their dispersion embedded within the ENR-50 matrix. Typical TEM micrographs for ENR-50/TiO$_2$ 10, 30, and 50 wt% are shown in Fig. 6a, b, and c respectively. Generally, the size of TiO$_2$ nanoparticles in the hybrid at 10 wt% TiO$_2$ was about 10–20 nm (Fig. 6a), while the size of TiO$_2$ nanoparticles in the hybrid at 30 wt% TiO$_2$ was about 25–40 nm (Fig. 6b). However, the higher TiO$_2$ content (50 wt%) showed a different behavior in the hybrid, the size of the TiO$_2$ here is unpredictable due to the sever agglomeration of these nanoparticles in the ENR-50 (Fig. 6c), this is also consistent with the results of the SEM.
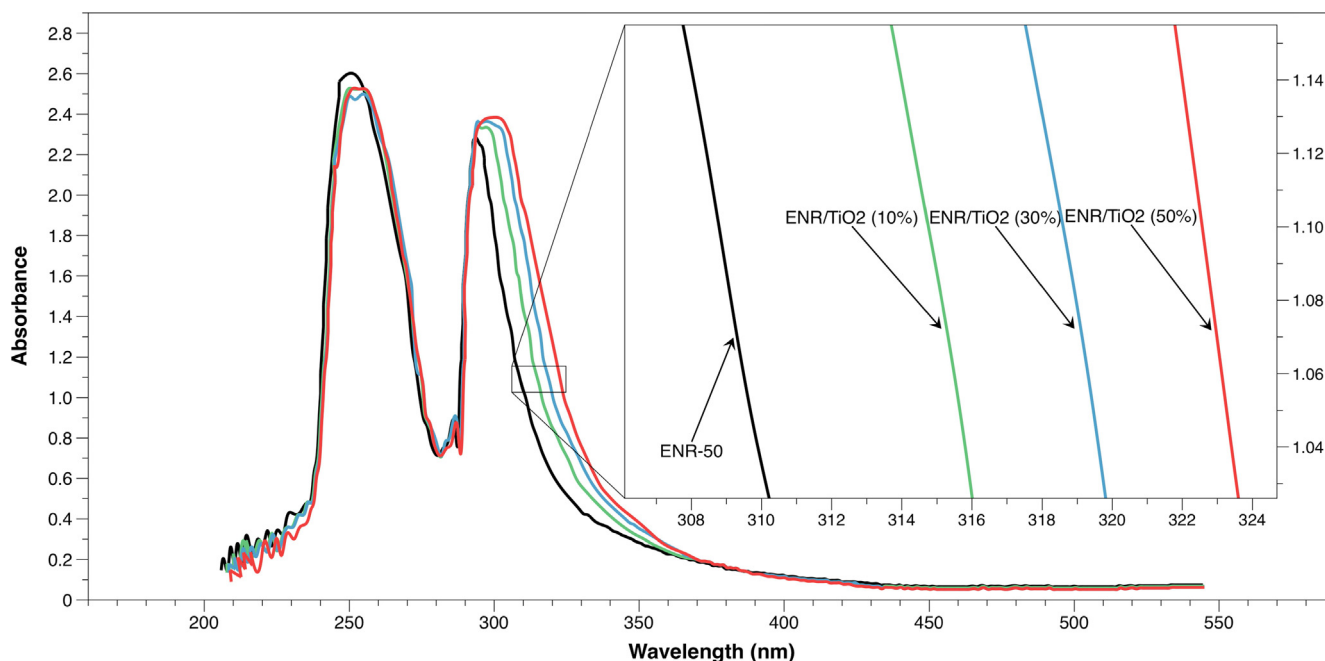
Fig. 8 UV–vis spectra of ENR-50 and ENR-50/TiO$_2$ at difference Ti Content.

3.6. Surface topography of nanocomposite films

Further insight on the surface topography of the ENR-50/TiO$_2$ hybrids was conducted using Atomic Force Microscopy (AFM) analysis. The three-dimension AFM micrographs of the ENR-50/TiO$_2$ hybrids at 10, 30, and 50 wt% titania are shown in Fig. 7a, b, and c respectively. These micrographs gave a clear understanding on the topographical variations of the hybrids. Based on the results, the hybrid at 10 wt% TiO$_2$ showed a smooth surface. However, the surface roughness of the hybrids gradually increased as titania content increase in the ENR-50 matrix indicating that more titania content are exist on the surfaces of the hybrid as more titania content are embedded (Mallakpour and Barati, 2011). Same changes were observed on the surface topography of acrylic resin/titania hybrids (Xiong et al., 2004), which is found that the surface roughness increased as titania content increase in the hybrid.

3.7. UV–Vis spectra identification and optical transparency

UV–vis absorption spectra of the ENR-50 and ENR-50/TiO$_2$ hybrid at 10, 30, and 50 wt% titania are illustrated in Fig. 8. It can be easily observed two absorption peaks at 250 nm and 293 nm appeared in ENR-50 sample. The peak at lower wavelength is associated with the π–π* transition of the carbon–carbon while the peak at lower wavelength is attributed to the n–π* transition of the nonbonding electron (loan pair electron of oxygen atom) of the epoxide groups (Mahmood et al., 2013). The two absorption peaks of the ENR-50 are have also appeared in all hybrid samples. The lower wavelength peak of all hybrid samples appeared at 251 nm while the higher wavelength peak appeared at 296–300 nm for the hybrid at 10, 30, and 50 wt% TiO$_2$. It can be clearly observed that the higher wavelength peak at 293 nm has shifted to 296,

298 and 300 nm for the hybrid at 10, 30, and 50 wt% TiO$_2$ respectively (Table 1), indicating that there is a significant interaction between titania precursors and ENR-50 matrix. Therefore, these results further support the observation of the ENR-50 - titania interaction, which increases with the increasing of titania content and maximum interaction occurs at 50 wt% titania. The nature of interaction between ENR-50 matrix and titania precursors was probably due to the ring opening reactions (ROR) of epoxide groups in ENR-50 and covalently bonded with the Ti moieties of titania resulting Ti-O bonds. This was explained clearly in the FTIR section of this work.

The optical transparency of the prepared ENR-50/TiO$_2$ hybrids was also investigated from the results of UV–visible spectroscopy. The optical transmissions of the samples were evaluated in the wavelength range of 200–550 nm (Fig. 8). The absorbance of the all hybrids started to became around zero after the 400 nm wavelength, which indicated a very good optical transparency in the visible light range. These results are consistent with the report studied the impact of TiO$_2$ on the optical transparency of Epoxy/TiO$_2$ nanocomposite films prepared by by sol–gel technique (Guan et al., 2006).

Table 1 Shift of wavelength of absorption peak due to n–π* transition of the nonbonding electron (loan pair electron of oxygen atom) of the epoxide groups with the variation of titania content.

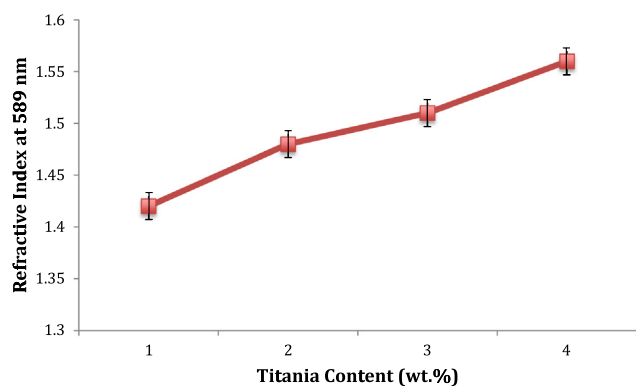| Sample	n–π* transition (nm) of the nonbonding electron of the epoxide groups
ENR-50	293
ENR/TiO$_2$ (10%)	296
ENR/TiO$_2$ (30%)	298
ENR/TiO$_2$ (50%)	300

Fig. 9 Refractive indices of ENR-50 and ENR-50/TiO$_2$ at difference Ti Content.

3.8. Refractive index

The refractive index of the ENR-50 matrix and ENR-50/TiO$_2$ hybrid at 10, 30, and 50 wt% TiO$_2$ are shown in Fig. 9. The refractive index of the pure ENR-50 sample was about 1.42 nm; wile the refractive index of the hybrid at 10, 30, and 50 wt% TiO$_2$ was about 1.48, 1.51, and 1.56 nm respectively. This indicated that the refractive index has linearly increased with the increase of titania content in the hybrid. These results are consistent with several reports that studied the influence of titania on the refractivity of the different polymer materials (Higashihara and Ueda, 2015; Nussbaumer et al., 2003; Liu et al., 2011). The increasing of refractive index of the hybrids was due to the dispersion and the interaction of titania network to ENR-50 matrix, which become stronger with the increase titania content. Moreover, the titania network has a high refractive index (about 2.2 nm) (Lü and Yang, 2009) which plays an essential role for the increasing of refractive index of hybrids. Therefore, it can be concluded that the refractive index of the hybrids can be attuned by selecting the suitable amount of titania.

4. Conclusion

A new organic–inorganic hybrid from ENR-50 and TiO$_2$ was successfully synthesized using sol–gel technique. It is found that the titania precursors have effectively bonded with the ring-opened epoxide units of ENR-50 forming covalent bond (Ti—O—C). This bonding has effected positively on the overall properties of the hybrid. This is in agreement with the microscopic analyses, which showed a good distribution of TiO$_2$ nanoparticles in ENR-50 matrix and also showed a strong interfacial bonding between matrix and nanoparticles. The presence of TiO$_2$ improved the optical transparency and also increased the refractive index of the hybrid. Therefore, this hybrid can be successfully used in the applications that require high refractive index such as micro optical and optoelectronic devices.

Declaration of Competing Interest

The authors declare that they have no known competing financial interests or personal relationships that could have appeared to influence the work reported in this paper.

References

Aakeröy, C.B., Beatty, A.M., Leinen, D.S., 1999. A versatile route to porous solids: organic–inorganic hybrid materials assembled through hydrogen bonds. Angew. Chem. Int. Ed. 38 (12), 1815–1819.

Akiba, M., Hashim, A.S., 1997. Vulcanization and crosslinking in elastomers. Prog. Polym. Sci. 22 (3), 475–521.

Bijarimi, M., Ahmad, S., Rasid, R., 2014. Mechanical, thermal and morphological properties of poly (lactic acid)/epoxidized natural rubber blends. J. Elastomers Plast. 46 (4), 338–354.

Brown, M.E., 2001. Introduction to Thermal Analysis: Techniques and Application. Kluwer Academic Publishers, The Netherlands.

Burroughes, J.H., Bradley, D.D.C., Brown, A.R., Marks, R.N., Mackay, K., Friend, R.H., et al, 1990. Light-emitting diodes based on conjugated polymers. Nature 347 (6293), 539.

Caldeira, L., Vasconcelos, D.C., Nunes, E.H., Costa, V.C., Musse, A. P., Hatimondi, S.A., Vasconcelos, W.L., 2012. Processing and characterization of sol–gel titania membranes. Ceram. Int. 38 (4), 3251–3260.

Chang, C.C., Chen, W.C., 2001. High-refractive-index thin films prepared from aminoalkoxysilane-capped pyromellitic dianhydride–titania hybrid materials. J. Polym. Sci., Part A: Polym. Chem. 39 (19), 3419–3427.

Chen, H.J., Jian, P.C., Chen, J.H., Wang, L., Chiu, W.Y., 2007. Nanosized-hybrid colloids of poly (acrylic acid)/titania prepared via in situ sol–gel reaction. Ceram. Int. 33 (4), 643–653.

Chen, W.C., Liu, W.C., Wu, P.T., Chen, P.F., 2004. Synthesis and characterization of oligomeric phenylsilsesquioxane-titania hybrid optical thin films. Mater. Chem. Phys. 83 (1), 71–77.

Çopuroğlu, M., O'Brien, S., Crean, G.M., 2006. Effect of preparation conditions on the thermal stability of an epoxy-functional inorganic–organic hybrid material system with phenyl side group. Polym. Degrad. Stab. 91 (12), 3185–3190.

Cui, Z., Lü, C., Yang, B., Shen, J., Su, X., Yang, H., 2001. The research on syntheses and properties of novel epoxy/polymercaptan curing optical resins with high refractive indices. Polymer 42 (26), 10095–10100.

Dahham, O.S., Hamzah, R., Bakar, M.A., Zulkepli, N.N., Ting, S.S., Omar, M.F., Adam, T., Muhamad, K., Dahham, S.S., 2018. Synthesis and structural studies of an epoxidized natural rubber/ titania (ENR-50/TiO2) hybrid under mild acid conditions. Polym. Test. 65, 10–20.

Dahham, O.S., Hamzah, R., Bakar, M.A., Zulkepli, N.N., Alakrach, A.M., Sam, S.T., Omar, M.F., Adam, T., Al-rashdi, A.A., 2020. Insight on the structural aspect of ENR-50/TiO2 hybrid in KOH/ C3H8O medium revealed by NMR spectroscopy. Arabian J. Chem. 13 (1), 2400–2413.

Di Gianni, A., Trabelsi, S., Rizza, G., Sangermano, M., Althues, H., Kaskel, S., Voit, B., 2007. Hyperbranched polymer/TiO$_2$ hybrid nanoparticles synthesized via an in situ sol–gel process. Macromol. Chem. Phys. 208 (1), 76–86.

Dou, L., Wong, A.B., Yu, Y., Lai, M., Kornienko, N., Eaton, S.W., Ginsberg, N.S., 2015. Atomically thin two-dimensional organic-inorganic hybrid perovskites. Science 349 (6255), 1518–1521.

Drisko, G.L., Sanchez, C., 2012. Hybridization in materials science–evolution, current state, and future aspirations. Eur. J. Inorg. Chem. 2012 (32), 5097–5105.

Gan, S.N., Hamid, Z.A., 1997. Partial conversion of epoxide groups to diols in epoxidized natural rubber. Polymer 38 (8), 1953–1956.

Gelling, I.R., Tinker, A.J., bin Abdul Rahman, H., 1991. Solubility parameters of epoxidised natural rubber.

Guan, C., Lü, C.L., Liu, Y.F., Yang, B., 2006. Preparation and characterization of high refractive index thin films of TiO2/epoxy resin nanocomposites. J. Appl. Polym. Sci. 102 (2), 1631–1636.

Hamzah, R., Bakar, M.A., Khairuddean, M., Mohammed, I.A., Adnan, R., 2012. A structural study of epoxidized natural rubber (ENR-50) and its cyclic dithiocarbonate derivative using NMR spectroscopy techniques. Molecules 17 (9), 10974–10993.

Hamzah, R., Bakar, M.A., Dahham, O.S., Zulkepli, N.N., Dahham, S. S., 2016. A structural study of epoxidized natural rubber (ENR-50) ring opening under mild acidic condition. J. Appl. Polym. Sci. 133 (43).

Higashihara, T., Ueda, M., 2015. Recent progress in high refractive index polymers. Macromolecules 48 (7), 1915–1929.

Ju, Y.G., Almuneau, G., Kim, T.H., Lee, B.W., 2006. Numerical analysis of high-index nano-composite encapsulant for light-emitting diodes. Jpn. J. Appl. Phys. 45 (4R), 2546.

Lee, L.H., Chen, W.C., 2001. High-refractive-index thin films prepared from trialkoxysilane-capped poly (methyl methacrylate)− titania materials. Chem. Mater. 13 (3), 1137–1142.

Li, S.D., Chen, Y., Zhou, J., Li, P.S., Zhu, C.S., Lin, M.L., 1998. Study on the thermal degradation of epoxidized natural rubber. J. Appl. Polym. Sci. 67 (13), 2207–2211.

Liu, B.T., Tang, S.J., Yu, Y.Y., Lin, S.H., 2011. High-refractive-index polymer/inorganic hybrid films containing high TiO2 contents. Colloids Surf., A 377 (1–3), 138–143.

Liu, J.G., Ueda, M., 2009. High refractive index polymers: fundamental research and practical applications. J. Mater. Chem. 19 (47), 8907–8919.

Lü, C., Yang, B., 2009. High refractive index organic–inorganic nanocomposites: design, synthesis and application. J. Mater. Chem. 19 (19), 2884–2901.

Ma, H., Jen, A.Y., Dalton, L.R., 2002. Polymer-based optical waveguides: materials, processing, and devices. Adv. Mater. 14 (19), 1339–1365.

Macwan, D.P., Dave, P.N., Chaturvedi, S., 2011. A review on nano-TiO2 sol–gel type syntheses and its applications. J. Mater. Sci. 46 (11), 3669–3686.

Mahmood, W.A.K., Khan, M.M.R., Azarian, M.H., 2013. Sol-gel synthesis and morphology, thermal and optical properties of epoxidized natural rubber/zirconia hybrid films. J. Non-Cryst. Solids 378, 152–157.

Mallkpour, S., Barati, A., 2011. Efficient preparation of hybrid nanocomposite coatings based on poly (vinyl alcohol) and silane coupling agent modified TiO2 nanoparticles. Prog. Org. Coat. 71 (4), 391–398.

Mas Haris, M.R.H., Raju, G., 2014. Preparation and characterization of biopolymers comprising chitosan-grafted-ENR via acid-induced reaction of ENR50 with chitosan. Express Polym. Lett. 8 (2).

Moore, J.P., Shumaker, J.A., Houtz, M.D., Sun, L., Khramov, A.N., Jones, J.G., 2012. Thermal and optical properties of novel polyurea/silica organic–inorganic hybrid materials. J. Sol-Gel Sci. Technol. 63 (1), 168–176.

Morselli, D., Bondioli, F., Sangermano, M., Messori, M., 2012. Photo-cured epoxy networks reinforced with TiO2 in-situ generated by means of non-hydrolytic sol–gel process. Polymer 53 (2), 283–290.

Motaung, T.E., Luyt, A.S., Thomas, S., 2011. Morphology and properties of NR/EPDM rubber blends filled with small amounts of titania nanoparticles. Polym. Compos. 32 (8), 1289–1296.

Nussbaumer, R.J., Caseri, W.R., Smith, P., Tervoort, T., 2003. Polymer-TiO2 nanocomposites: A route towards visually transparent broadband UV filters and high refractive index materials. Macromol. Mater. Eng. 288 (1), 44–49.

Olshavsky, M.A., Allcock, H.R., 1995. Polyphosphazenes with high refractive indices: synthesis, characterization, and optical properties. Macromolecules 28 (18), 6188–6197.

Peng, Z., 2004. Rational synthesis of covalently bonded organic–inorganic hybrids. Angew. Chem. Int. Ed. 43 (8), 930–935.

Ratnam, C.T., Nasir, M., Baharin, A., Zaman, K., 2000a. Electron beam irradiation of epoxidized natural rubber: FTIR studies. Polym. Int. 49 (12), 1693–1701.

Ratnam, C.T., Nasir, M., Baharin, A., Zaman, K., 2000b. Electron beam irradiation of epoxidized natural rubber. Nucl. Instrum. Methods Phys. Res., Sect. B 171 (4), 455–464.

Ratnam, C.T., Nasir, M., Baharin, A., Zaman, K., 2001c. The effect of electron beam irradiation on the tensile and dynamic mechanical properties of epoxidized natural rubber. Eur. Polym. J. 37 (8), 1667–1676.

Rawolle, M., Niedermeier, M.A., Kaune, G., Perlich, J., Lellig, P., Memesa, M., Cheng, Y.J., Gutmann, J.S., Müller-Buschbaum, P., 2012. Fabrication and characterization of nanostructured titania films with integrated function from inorganic–organic hybrid materials. Chem. Soc. Rev. 41 (15), 5131–5142.

Salaeh, S., Nakason, C., 2012. Influence of modified natural rubber and structure of carbon black on properties of natural rubber compounds. Polym. Compos. 33 (4), 489–500.

Salehabadi, A., Bakar, M.A., Bakar, N.H.H.A., 2014. Effect of organo-modified nanoclay on the thermal and bulk structural properties of poly (3-hydroxybutyrate)-epoxidized natural rubber blends: Formation of multi-components biobased nanohybrids. Materials 7 (6), 4508–4523.

Schnabel, W., 1981. Polymer degradation: principles and practical applications.

Su, H.W., Chen, W.C., 2008. High refractive index polyimide–nanocrystalline-titania hybrid optical materials. J. Mater. Chem. 18 (10), 1139–1145.

Tan, W.L., Bakar, M.A., 2013. Synthesis, characterization and impedance spectroscopy study of magnetite/epoxidized natural rubber nanocomposites. J. Alloy. Compd. 561, 40–47.

Tanaka, K., Kozuka, H., 2004. Sol–gel preparation and mechanical properties of machinable cellulose/silica and polyvinylpyrrolidone/silica composites. J. Sol-Gel Sci. Technol. 32 (1–3), 73–77.

Wang, B., Wilkes, G.L., Hedrick, J.C., Liptak, S.C., McGrath, J.E., 1991. New high-refractive-index organic/inorganic hybrid materials from sol-gel processing. Macromolecules 24 (11), 3449–3450.

Wang, M.S., Xu, G., Zhang, Z.J., Guo, G.C., 2010. Inorganic–organic hybrid photochromic materials. Chem. Commun. 46 (3), 361–376.

Xiong, M., You, B., Zhou, S., Wu, L., 2004. Study on acrylic resin/titania organic–inorganic hybrid materials prepared by the sol–gel process. Polymer 45 (9), 2967–2976.

Yu, Y.Y., Rao, Y.C., Chang, C.C., 2013. Preparation and characterization of highly transparent epoxy/inorganic nanoparticle hybrid thin films. Thin Solid Films 546, 236–241.

Zhang, H., Qi, R., Tong, M., Su, Y., Huang, M., 2012. In situ solvothermal synthesis and characterization of transparent epoxy/TiO2 nanocomposites. J. Appl. Polym. Sci. 125 (2), 1152–1160.

Zimmennann, L., Weibel, M., Caseri, W., Suter, U.W., 1993. High refractive index films of polymer nanocomposites. J. Mater. Res. 8 (7), 1742–1748.